

HMSViT: A Hierarchical Masked Self-Supervised Vision Transformer for Corneal Nerve Segmentation and Diabetic Neuropathy Diagnosis

Xin Zhang, Liangxiu Han*, Yue Shi, Yanlin Zheng, Uazman Alam, Maryam Ferdousi and Rayaz Malik

Abstract—Diabetic Peripheral Neuropathy (DPN) affects nearly half of diabetes patients, requiring early detection. Corneal Confocal Microscopy (CCM) enables non-invasive diagnosis, but automated methods suffer from inefficient feature extraction, reliance on handcrafted priors, and data limitations. We propose HMSViT, a novel Hierarchical Masked Self-Supervised Vision Transformer (HMSViT) designed for corneal nerve segmentation and DPN diagnosis. Unlike existing methods, HMSViT employs pooling-based hierarchical and dual attention mechanisms with absolute positional encoding, enabling efficient multi-scale feature extraction by capturing fine-grained local details in early layers and integrating global context in deeper layers, all at a lower computational cost. A block-masked self supervised learning framework is designed for the HMSViT that reduces reliance on labelled data, enhancing feature robustness, while a multi-scale decoder is used for segmentation and classification by fusing hierarchical features. Experiments on clinical CCM datasets showed HMSViT achieves state-of-the-art performance, with 61.34% mIoU for nerve segmentation and 70.40% diagnostic accuracy, outperforming leading hierarchical models like the Swin Transformer and HiViT by margins of up to 6.39% in segmentation accuracy—while using fewer parameters. Detailed ablation studies further reveal that integrating block-masked SSL with hierarchical multi-scale feature extraction substantially enhances performance compared to conventional supervised training. Overall, these comprehensive experiments confirm that HMSViT delivers excellent, robust, and clinically viable results, demonstrating its potential for scalable deployment in real-world diagnostic applications.

Index Terms—Diabetic Peripheral Neuropathy (DPN), Corneal Confocal Microscopy (CCM), Vision Transformer, Self-Supervised Learning (SSL), Hierarchical Multi-Scale Learning

This work forms part of EPSRC funded project (EP/X013707/1 and EP/X01441X/1)

Xin Zhang, Liangxiu Han and Yue Shi are with the Department of Computing, and Mathematics, Manchester Metropolitan University, Manchester M15GD, U.K (e-mail: x.zhang@mmu.ac.uk; l.han@mmu.ac.uk; y.shi@mmu.ac.uk)

Yanlin Zheng and Uazman Alam are with Department of Eye and Vision Sciences, University of Liverpool, Liverpool L78TX, U.K (e-mail: yalin.zheng@liverpool.ac.uk; ualam@liverpool.ac.uk).

Maryam Ferdousi is with the Faculty of Biology, Medicine and Health, University of Manchester, Manchester, U.K (e-mail: maryam.ferdousi@manchester.ac.uk).

Rayaz Malik is with Department of Medicine, Weill Cornell Medicine-Qatar, Doha, Qatar (e-mail: ram2045@qatar-med.cornell.edu).

I. INTRODUCTION

DIABETIC Peripheral Neuropathy (DPN) is a debilitating complication of diabetes, affecting nearly 50% of individuals with diabetes worldwide and significantly increasing the risk of foot ulcers, infections, and lower-limb amputations [1]. This progressive neurodegenerative condition is characterized by nerve damage, primarily in the peripheral nervous system, leading to symptoms such as pain, numbness, and loss of sensation in the extremities. Early diagnosis and continuous monitoring are essential to mitigate its impact and prevent irreversible nerve damage.

However, traditional diagnostic methods, including nerve conduction studies and skin biopsies, are invasive, costly, and often unsuitable for routine screening [2]. In recent years, Corneal Confocal Microscopy (CCM) has emerged as a non-invasive and highly sensitive imaging modality for early DPN detection [3]. CCM enables high-resolution imaging of corneal nerve fibres, which serve as quantifiable biomarkers for neuropathy progression. Despite its potential, the manual analysis of CCM images is time-consuming, prone to inter-observer variability, and requires expert interpretation, making it impractical for large-scale screening [4], [5]. These challenges underscore the need for automated, AI-driven solutions that can efficiently analyse CCM images for both corneal nerve segmentation and DPN severity classification.

The advent of deep learning has significantly advanced medical image analysis, with Convolutional Neural Networks (CNNs) being widely adopted for automated segmentation and classification [6], [7]. While CNNs are exceptional at extracting hierarchical feature representations, their fixed local receptive fields can hinder the capture of long-range dependencies and global structural variations—an essential factor in accurately interpreting complex nerve fibre morphology [7]. To overcome these constraints, Vision Transformers (ViTs) [8] have emerged as a potent alternative, employing self-attention mechanisms to harness global contextual information, which is particularly advantageous for medical imaging tasks requiring fine-grained structural recognition [9].

Nonetheless, standard ViTs face notable challenges in medical imaging, especially for tasks demanding high-resolution representations, such as organ segmentation or nerve fibre

analysis [9], [10]. Firstly, ViTs require extensive annotated datasets, which are often unavailable in medical contexts, and their patch-based processing reduces spatial resolution and lacks inductive bias for spatial reasoning - the ability to understand structure and relationships within an image. These limitations call for innovative solutions to harness ViTs' strengths while addressing their shortcomings.

Prior studies have explored hierarchical Vision Transformer architectures, such as the Swin Transformer [11] and HiViT [12] that progressively merge patches to extract multi-scale features, thereby capturing both local detail and global context. However, these methods often depend on handcrafted modules (e.g., shifted windows or convolutional enhancements) that increase computational complexity. In parallel, self-supervised learning (SSL) techniques, notably masked autoencoders, have been applied to alleviate the dependency on large labelled datasets, although integrating SSL with hierarchical models remains challenging.

To address these issues, we propose HMSViT—a Hierarchical Masked Self-Supervised Vision Transformer. HMSViT employs a pooling-based hierarchical design with dual attention mechanisms, where early layers capture fine-grained local details and deeper layers integrate global contextual information using absolute positional encodings. A novel block-masked SSL approach is introduced to learn robust spatial relationships from unlabelled CCM images, reducing reliance on extensive annotations. A multi-scale decoder further fuses these features for both accurate corneal nerve segmentation and DPN diagnosis. In summary, our contributions are threefold:

- 1) **Efficient Multi-Scale Feature Extraction:** A pooling-based hierarchical design with dual attention effectively captures both local and global features without heavy reliance on handcrafted modules.
- 2) **Innovative Self-Supervised Learning:** A block-masked SSL approach tailored for hierarchical architectures improves spatial reasoning while minimizing computational overhead.
- 3) **State-of-the-Art Clinical Performance:** HMSViT demonstrates superior segmentation accuracy and diagnostic classification on clinical CCM datasets, offering a scalable, non-invasive solution for early DPN screening.

II. RELATED WORK

A. Epidemiological Context and Clinical Need

Diabetes affects 463 million people worldwide, projected to reach 700 million by 2045 [13]. Diabetic Peripheral Neuropathy (DPN), impacting up to 50% of patients, causes 50–75% of non-traumatic lower-limb amputations [14]. Defined as peripheral nerve dysfunction in diabetes after excluding other causes [15], DPN highlights the urgent need for early detection to prevent irreversible damage.

Corneal Confocal Microscopy (CCM) is a non-invasive tool for early DPN detection, allowing quantitative analysis of the corneal sub-basal nerve plexus, which is highly sensitive to metabolic damage [16]. Manual annotation of CCM images is time-consuming, expertise-dependent, and subject to variability due to noise and interpretation bias [5]. These limitations

have led to the development of automated methods to extract key diagnostic metrics, including corneal nerve fibre length (CNFL), density (CNFD), and branch density (CNBD).

B. Deep Learning Methods for Corneal Nerve Segmentation and DPN Diagnosis

Recent advancements in deep learning have significantly improved automated CCM image analysis, particularly in the areas of corneal nerve segmentation and DPN classification. The most prominent approaches include Convolutional Neural Networks (CNNs) and Vision Transformers (ViTs), both of which have demonstrated success in various medical imaging applications.

1) **CNN-Based Approaches:** CNNs have been extensively used for DPN classification and corneal nerve segmentation, leveraging their ability to capture hierarchical spatial features. Several CNN-based approaches have been explored in recent years. [17] developed a CNN-based classifier for DPN detection using CCM images, incorporating data augmentation techniques to improve model generalisation. Similarly, [18] applied ResNet architectures, achieving high classification accuracy in identifying neuropathic changes. For segmentation, [19] employed U2Net to precisely quantify corneal nerve fibre parameters, significantly enhancing the sensitivity of DPN detection. [7] further demonstrated that CNN-based segmentation approaches could outperform traditional corneal nerve analysis software (e.g., ACC Metrics), providing more accurate and reliable quantification of nerve fibre morphology. In addition, [20] implemented a 3D CNN model to classify painful DPN subtypes, highlighting the potential of CNNs in personalized medicine and treatment response analysis.

Despite their effectiveness, CNN-based approaches are fundamentally constrained by fixed local receptive fields, limiting their ability to model long-range dependencies and complex nerve fibre branching patterns. Since CNNs rely on localized feature extraction, they struggle to capture the global structure of corneal nerve morphology, which is critical for accurate segmentation. Additionally, CNN-based models are highly sensitive to image contrast variations and noise, making their performance inconsistent across different datasets. These limitations have led researchers to explore Vision Transformers (ViTs), which leverage self-attention mechanisms to capture both local and global spatial dependencies.

2) **Vision Transformers (ViTs):** ViTs have gained increasing attention in medical imaging due to their ability to model global spatial relationships. Unlike CNNs, which process images through localized convolutional operations, ViTs divide images into patches and apply self-attention mechanisms across the entire image, enabling them to capture long-range dependencies [9]. This global view is critical for accurately identifying and segmenting nerve fibres that often extend over large parts of CCM images [8].

Several studies have explored ViT-based models for corneal nerve segmentation and DPN classification. [21] introduced a ViT-based context encoder that integrates channel-wise attention mechanisms, improving segmentation accuracy by preserving subtle nerve fibre structures. Similarly, [22] applied

a transformer-based classifier for DPN detection, demonstrating higher diagnostic accuracy compared to CNN-based approaches. While ViTs offer advantages in modeling global context, they suffer from limitations. The patch-based tokenisation in ViTs results in spatial resolution loss, making them less effective for dense segmentation tasks such as nerve fibre analysis.

To address the limitations of standard ViTs, Hierarchical Vision Transformers (HVTs) introduce multi-scale feature extraction, progressively refining spatial resolution through patch merging and downsampling. Table I provides a concise comparison between standard ViTs and Hierarchical ViTs. Standard ViTs process images with fixed-size patches across all layers, resulting in uniform tokenisation. While effective, this approach leads to quadratic computational complexity and requires large datasets for training. In contrast, Hierarchical ViTs use progressive patch merging and downsampling. This reduces computational cost and enables multi-scale feature learning. As a result, HVTs capture both local and global structures efficiently and often generalise better on smaller datasets by leveraging spatial hierarchies.

Several hierarchical transformer architectures have been developed for medical image segmentation. The Swin Transformer [11] introduced shifted window attention, balancing local and global feature representation while reducing computational complexity. The HiViT model [12] refined hierarchical tokenisation, demonstrating that simpler architectures could achieve competitive segmentation performance. The MViTv2 [26] framework improved multi-scale learning by integrating decomposed positional embeddings and residual pooling, allowing for more efficient spatial relationship modeling.

Despite these promising developments, the application of hierarchical vision transformers (HVTs) in medical imaging remains challenging. Although HVTs offer multi-scale representation, they typically depend on spatial priors such as convolutions [12], shifted windows [11], and intricate relative position embeddings to introduce spatial bias into the model [27]. While these mechanisms improve supervised task accuracy, they also increase computational complexity, reduce inference speed, and complicate the integration of efficient self-supervised tasks.

Moreover, no existing studies have explored the application of HVTs for corneal confocal microscopy (CCM) image segmentation or DPN diagnosis, leaving a critical gap in leveraging their potential for medical imaging tasks. Additionally, the reliance on large-scale annotated datasets for effective pretraining presents a major obstacle in medical applications, where labelled data is often scarce, costly, and time-consuming to obtain. To address these limitations, recent efforts have focused on integrating self-supervised learning (SSL) techniques with vision transformer architectures. SSL enables models to learn robust spatial representations from abundant unannotated data, significantly reducing their dependency on manual annotations and improving their adaptability to medical imaging tasks.

C. Self-Supervised Learning (SSL)

Self-supervised learning (SSL) has become essential in computer vision, enabling models to learn robust representa-

tions from large unlabelled datasets. This approach is particularly valuable for Vision Transformers (ViTs), which require extensive data to achieve competitive performance compared to convolutional neural networks [28]. SSL methods rely on pretext tasks such as predicting missing image parts or distinguishing between different augmented views of an image [29], helping models capture spatial and semantic information without labelled data.

Early SSL methods introduced tasks including context prediction [30], inpainting [31], solving jigsaw puzzles [32], and rotation prediction [33], laying a foundation for more advanced techniques. Later, contrastive approaches like SimCLR [34] and MoCo [35] further improved SSL by learning representations that align similar views and separate unrelated images.

Recently, masked autoencoders (MAE) [36] advanced SSL for ViTs by masking image patches and training models to reconstruct the missing pixels, efficiently capturing both global and fine-grained image details. Empirical results demonstrate that MAE accelerates training and achieves superior performance in benchmark tasks, including ImageNet classification and dense prediction, surpassing traditional SSL approaches [27].

Several attempts have been made to integrate masked SSL into hierarchical ViTs. Approaches such as MaskFeat [37], MixMAE [38], and Fast-iTPN [39] tackle this challenge by processing masked patches using specialised masked tokens. However, these methods often incur substantial computational overhead because a large portion of computation is devoted to masked tokens, which slows down training.

In contrast, we present block masked self-supervised learning for hierarchical ViT pretraining, resulting in a model that is both powerful and efficient.

III. THE PROPOSED METHOD

In this work, we introduce HMSViT—a hierarchical vision transformer for automated corneal nerve segmentation and DPN classification (Figure 1). Its design centers on three components:

- 1) **Hierarchical Multi-Scale Feature Extraction:** HMSViT processes images through four stages, starting with high-resolution inputs to capture fine details and gradually reducing spatial resolution to extract higher-level features. Instead of relying on complex modules (e.g., shifted windows or convolutions), our design uses a non-parametric pooling operator, with block-based local attention in early stages and global attention in deeper stages complemented by block-level absolute positional encodings.
- 2) **Block Masked Self-Supervised Learning:** To learn robust spatial relationships without heavy labelled data, we adapt a Block masked SSL approach. Rather than masking individual patches, we group 4×4 patches into larger 16×16 blocks, aligning with the hierarchical structure and reducing computational overhead.
- 3) **Multi-Scale Decoder:** A multi-scale decoder fuses hierarchical features for downstream tasks, enabling effective corneal nerve segmentation and diabetic neuropathy diagnosis.

	Standard Vision Transformer (ViT)	Hierarchical Vision Transformer (HVT)
Patch Handling	Fixed-size patches across all layers	Progressive patch merging & down sampling
Compute Complexity	Quadratic in image resolution	Reduced complexity with hierarchical tokenisation
Feature Extraction	Uniform token processing	Multi-scale feature learning (local to global)
Examples	Original ViT [8], DeiT [23], DPT [24]	Swin Transformer [11], PVT [25], HiVi [12]
Performance	Performs well on image classification, especially with large datasets and pretraining.	Often achieves better performance on dense prediction tasks like object detection and semantic segmentation due to multi-scale feature representation.

TABLE I

COMPARISON OF STANDARD VISION TRANSFORMER (ViT) AND HIERARCHICAL VISION TRANSFORMER (HVT) ARCHITECTURES.

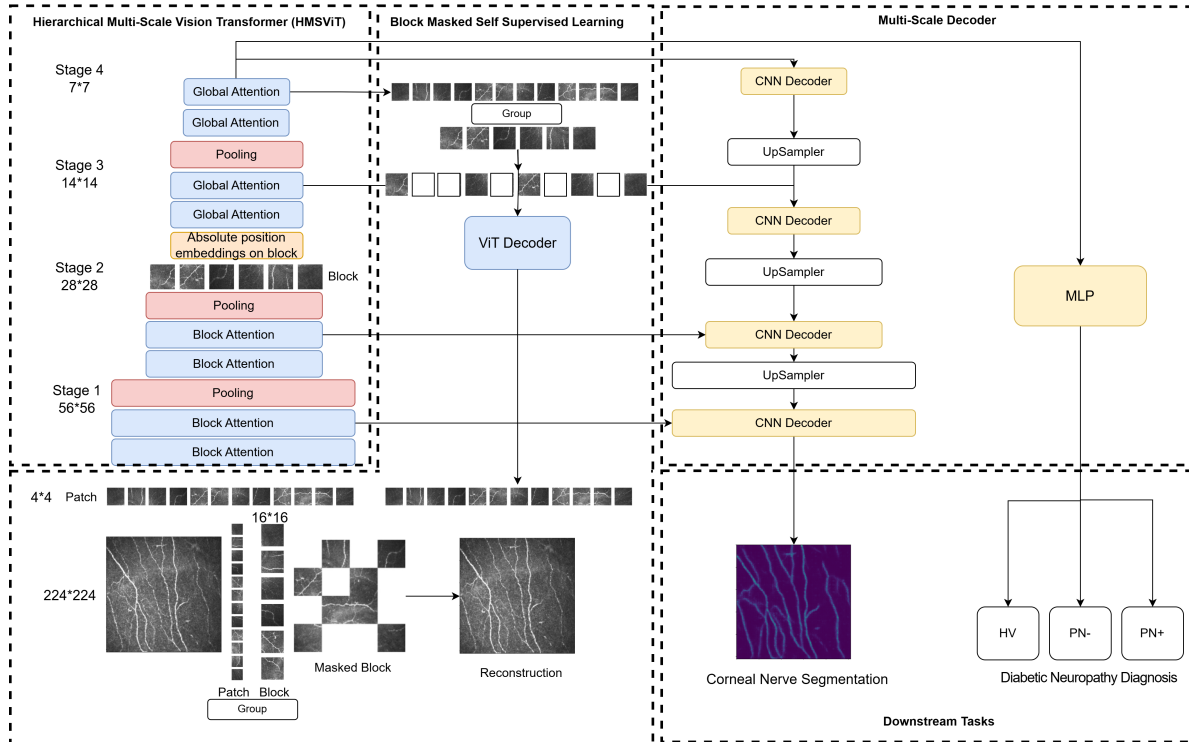


Fig. 1. Overview of the proposed method. 1) HMSViT is designed to learn multi-scale representations across four stages through pooling based dual attention mechanisms; 2) A block masked self-supervised learning is used to pretrain the HMSViT to enhance the model’s spatial reasoning by reconstructing masked input blocks; 3) A multi-scale decoder is designed for downstream tasks including corneal nerve segmentation and Diabetic neuropathy diagnosis.

A. Hierarchical Multi-Scale Vision Transformer (HMSViT)

The proposed method leverages the strengths of Vision Transformers (ViTs) while addressing their limitations in dense medical imaging tasks—specifically, for corneal nerve fibre segmentation and Diabetic Peripheral Neuropathy (DPN) diagnosis. By progressively extracting features at multiple scales, the network captures both fine-grained local details and broader global context, leading to enhanced segmentation performance and improved diagnostic accuracy.

1) *High-Resolution Hierarchical Representations*: First, for an input image $X \in \mathbb{R}^{H \times W \times C}$, where H and W are the height and width of the input image and C is the number of channels. HMSViT employs a small patch size of 4×4 to obtain high-resolution feature maps. This results in a feature map of size 56×56 when using a 224×224 input image. Then each patch is flattened and linearly embedded to generate a token representation:

$$X_p = \text{PatchEmbed}(X) \in \mathbb{R}^{L \times d}, \quad (1)$$

where $L = \frac{H}{p} \times \frac{W}{p}$ is the number of patches, p is the patch size. d is the feature dimension. $\frac{H}{p} \times \frac{W}{p}$ is the output feature size.

Since the computational complexity of a ViT scales quadratically with the number of tokens (i.e., $O(L^2)$), it becomes essential to reduce the number of tokens to decrease computation and enable multi-scale representations. The patch tokens are first rearranged into a new unit called a Block (B). At a given stage l , the tokens are grouped into blocks:

$$B^l = \text{Concat}\{X_1, X_2, X_3, \dots, X_{16}\} \in \mathbb{R}^{4 \times 4 \times d} \quad (2)$$

A non-parametric max pooling operator is then applied to each block to downsample the representation while preserving the most salient features. The pooling operation is defined as:

$$B^{(l+1)} = \text{MaxPool}(B^l) \quad (3)$$

This operation reduces the spatial resolution and aggregates the most dominant features, facilitating efficient hierarchical feature extraction.

2) *Dual Attention Mechanisms*: Given that high-resolution features in the early stages result in $L = \frac{H}{p} \times \frac{W}{p}, p = 4$, applying global self-attention becomes computationally intensive due to its $O(L^2)$ complexity. To mitigate this, HMSViT employs a dual attention strategy tailored to different stages of the network.

$$\text{Attention} = \text{softmax} \left(\frac{QK^T}{\sqrt{d}} \right) V \quad (4)$$

- **Block-based Attention** in early stages, where attention is computed within local blocks of 16 patches.
- **Global Attention** in deeper stages, as the spatial dimensions reduce, the model switches to global attention to integrate high-level semantic information across the entire image.

3) *Absolute Positional encodings*: To preserve spatial relationships—crucial in medical imaging—we add positional encodings to the input data. While standard ViTs use absolute or relative embeddings (with hierarchical models often favoring relative ones for consistency across varying resolutions), relative embeddings require modifying the attention mechanism and add computational overhead. In our method, we simply add learnable absolute positional encodings at the block level in deeper stages:

$$\tilde{B}^l = B^l + p^l \quad (5)$$

where p^l is the learnable absolute positional embedding for token l .

B. Block Masked self-supervised learning

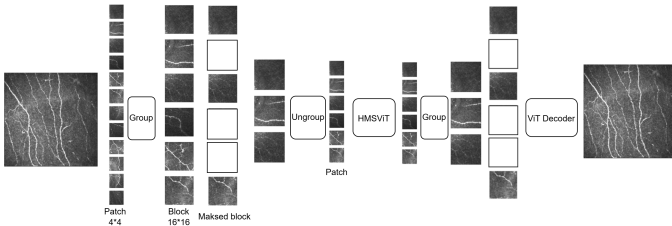


Fig. 2. Block Masked Self Supervised Learning

Our approach builds on the recent advances in Masked Autoencoders (MAE) [36], where a large portion of the input (typically 75–90%) is masked out, and the model is trained to reconstruct the missing parts. This strategy forces the network to learn rich spatial relationships, as it must infer the structure of the masked regions from the visible context. However, in a hierarchical Vision Transformer (ViT) with progressive downsampling, directly applying standard MAE can disrupt spatial coherence across scales. To address this, we propose a block-masking strategy that groups small patches (e.g., 4×4 patches) into larger block units before masking. As shown in Figure 2, we (1) group the patches into block units, (2) randomly mask blocks at the block level, and (3) ungroup them back into smaller patches for our HMSViT.

Given an input feature map X , a binary mask $M \in \{0, 1\}^N$ is generated, where: $X_{\text{unmasked}} = (1 - M) \odot X$, \odot denotes

element-wise multiplication. Then the visible blocks are fed into HMSViT:

$$\hat{F} = \text{HMSViT}(X_{\text{unmasked}}) \quad (6)$$

The decoder takes the latent representation (\hat{F}) and, typically, a set of learnable mask tokens to reconstruct the full input:

$$\hat{X} = \text{Decoder}(\hat{F}, \text{masked block tokens}) \quad (7)$$

The training objective is to minimize the reconstruction error, but only over the masked blocks. The masked autoencoder loss is:

$$\mathcal{L} = \mathbb{E}_{x \sim p(x)} \left[\|(1 - M) \odot (x - \hat{X})\|^2 \right] \quad (8)$$

where the loss is computed only over the positions where M indicates a mask (i.e., $1 - M$ selects the masked regions).

C. Multi-scale decoder

We introduce a multi-scale decoder that fuses HMSViT’s hierarchical features for both corneal nerve segmentation and DPN diagnosis.

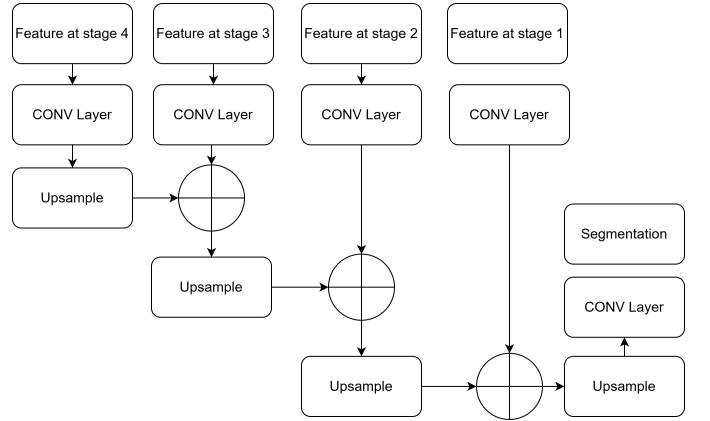


Fig. 3. Multi-scale decoder

For segmentation, as shown in Figure 3, the hierarchical features F_i from different stages are fused. Let $U(\cdot)$ be an upsampling function that brings features to a common resolution. The fused feature map is computed as:

$$y_{\text{seg}} = \sigma \left(\sum_i U(F_i) \right) \quad (9)$$

where $\sigma(\cdot)$ denotes a convolution with activation functions to refine the aggregated representation.

For classification (e.g., DPN diagnosis), the lowest-resolution feature F_{global} is fed to an MLP:

$$y_{\text{classification}} = \text{MLP}(F_{\text{global}}) \quad (10)$$

IV. EXPERIMENTAL EVALUATION

A. Experimental Design

The experiments in this study are designed to evaluate the effectiveness and efficiency of our proposed self-supervised HMSViT across multiple tasks, focusing on diabetic peripheral neuropathy (DPN) diagnosis and segmentation of corneal nerve fibres. Three main experiments are conducted:

1) *Task 1: Model Performance Evaluation*: We evaluate HMSViT on two tasks—DPN diagnosis and corneal nerve fibre segmentation—by comparing three configurations (Tiny, Small, Base) with state-of-the-art models (Swin Transformer [11] and HiViT [12]).

- 1) **DPN Diagnosis Task**: In this task, models are trained to classify participants into three categories: Healthy Volunteers (HV), Diabetic Patients without Peripheral Neuropathy (PN−), and Diabetic Patients with Peripheral Neuropathy (PN+). Performance is evaluated using metrics such as accuracy, precision, recall, and F1-score to provide a comprehensive assessment of diagnostic reliability. Comparisons between HMSViT and the baseline models reveal improvements in classification performance, highlighting the effectiveness of HMSViT in accurately diagnosing DPN.
- 2) **Corneal Nerve fibre Segmentation Task**: This task evaluates the models’ ability to accurately identify and delineate corneal nerve fibres. The primary metric is the mean Intersection over Union (mIoU), which measures the overlap between predicted and actual segmentation regions. In addition, clinically relevant metrics (Table II)—Corneal Nerve fibre Length (CNFL) and Corneal Nerve Branch Density (CNBD)—are used to quantify nerve morphology, offering further insights into early DPN detection. The results underscore HMSViT’s superior segmentation accuracy compared to existing hierarchical vision transformers.

Parameter	Description	Unit of Measurement
Corneal nerve fibre length (CNFL)	Length of all main nerve fibres and branches	mm/mm ²
Corneal nerve branch density (CNBD)	Number of main nerve fibre branches	no/mm ²

TABLE II

PARAMETERS FOR CORNEAL NERVE FIBRE ANALYSIS.

2) *Task 2: Ablation Study to Evaluate the Impact of Hierarchical Design and Self-Supervised Learning*: An ablation study is conducted to assess the impact of key components of the proposed model: 1) Hierarchical Design and 2) Self-Supervised Learning. The experiment is divided into four settings: (1) supervised training without the hierarchical structure, (2) supervised training with the hierarchical structure, (3) SSL without the hierarchical structure, and (4) SSL with the hierarchical structure.

3) *Task 3: Comparison with State-of-the-Art Methods for Segmentation*: To comprehensively evaluate HMSViT’s segmentation performance, we compare it against several state-of-the-art transformer-based models, including standard Vision Transformers (ViTs), hierarchical ViTs, and self-supervised learning (SSL) approaches (Table III). This evaluation spans diverse architectural paradigms, ranging from vanilla transformers to hierarchical and convolutional variants, ensuring a thorough comparison of model effectiveness.

For a comprehensive performance assessment, we use evaluation metrics including mean Intersection over Union (mIoU), a widely adopted metric in segmentation tasks. In this experiment, we focused exclusively on corneal nerve segmentation results because precise nerve delineation is fundamental to both clinical assessment and the overall performance of our

system. Accurate segmentation directly impacts the quantification of clinically relevant parameters—such as nerve fibre length and branch density—which are critical for diagnosing diabetic peripheral neuropathy. Moreover, most of the hierarchical models we compare are specifically designed for segmentation tasks, ensuring that our evaluation is both fair and directly aligned with the core functionality of these architectures.

B. Datasets

We employ two main datasets to train and evaluate HMSViT. This section details the acquisition, characteristics, and role of these datasets in our experiments. First, a larger, diverse collection of CCM images supports our self-supervised pretraining, enabling robust feature learning from unlabelled data. Second, a clinical dataset of corneal confocal microscopy (CCM) images—captured from both healthy volunteers and diabetic patients with or without peripheral neuropathy—is used for nerve segmentation and DPN diagnosis.

1) *Datasets for self-supervised pretraining*: In this work, a total of 6,426 eye CCM images from different sources were collected for block masked self-supervised learning pretrain (Table IV).

2) *Datasets for Corneal Nerve Segmentation and Diabetic Neuropathy Diagnosis*: The dataset used in this study, provided by the Early Neuropathy Assessment (ENA) group from the University of Manchester, UK, consisted of images of the corneal sub basal nerve plexus. These images were sourced from healthy volunteers (HV) and participants with either pre-diabetes or diabetes, encompassing a total of 184 individuals.

Each participant had up to seven CCM images. The corneal confocal microscopy (CCM) images were obtained using an internationally recognized protocol developed by the ENA group. The imaging was conducted with the Rostock Corneal Module of a Heidelberg Retina Tomograph III confocal laser microscope (HRTIII32-RCM, Heidelberg Engineering, Germany) at a resolution of 400×400 μm (384 × 384 pixels). The images were exported in BMP file format to ensure compatibility with the image analysis software.

The participants were categorised into different groups: Healthy Volunteers (HV): 112 patients (35.2%), no diabetes or neuropathy. Diabetic Patients without Neuropathy (PN−): 98 patients (30.8%), diabetes duration ≥ 5 years. Diabetic Patients with Neuropathy (PN+): 108 patients (34.0%), confirmed DPN symptoms. Meanwhile, we also annotated the fibre with branching by expert for the segmentation task. Figure 4 shows example CCM images and the manual annotation, with branching highlighted.

V. RESULT

A. Model Performance Evaluation

We evaluated HMSViT on corneal nerve segmentation and diabetic neuropathy (DPN) diagnosis using three configurations (Tiny, Small, Base) and compared its performance with Swin Transformer [11] and HiViT [12].

Overall Performance: Table V shows that HMSViT consistently outperforms Swin and HiViT in both segmentation

Category	Method	Description
Baseline Vision Transformer	DPT [24]	A ViT-based model designed specifically for dense prediction tasks like segmentation.
	HiViT [12]	Extends ViT by incorporating multi-scale feature representations.
Hierarchical Vision Transformers	PoolFormer [40]	Replaces traditional self-attention with pooling operations to efficiently capture contextual information.
	SegFormer [41]	A transformer optimised for semantic segmentation, with a focus on efficient multi-scale feature aggregation.
	Fast-iTPN [39]	A pyramid-based architecture that enhances efficiency and downstream performance by integrating token migration and gathering while jointly pretraining both the backbone and the neck.
Self-Supervised Learning Approaches	MoCo v3 [42]	Utilises contrastive learning to learn robust visual representations.
	MAE [36]	Implements a masked autoencoder strategy to reconstruct missing regions, improving feature learning.
	MixMIM [38]	Enhances MAE by introducing a mixing strategy, replacing masked tokens with tokens from another image to encourage richer feature disentanglement.

TABLE III

COMPARISON OF VISION TRANSFORMER ARCHITECTURES AND SELF-SUPERVISED LEARNING APPROACHES.

Dataset	Description	Count
CORN-1	Nerve segmentation subset	1698
CORN-2	Image enhancement subset	688
CORN-3	Nerve tortuosity grading	403
CORN1500	Extended tortuosity grading	1500
UoM CCM	Diabetes classification dataset	2137

TABLE IV

DATASETS FOR SELF-SUPERVISED LEARNING.

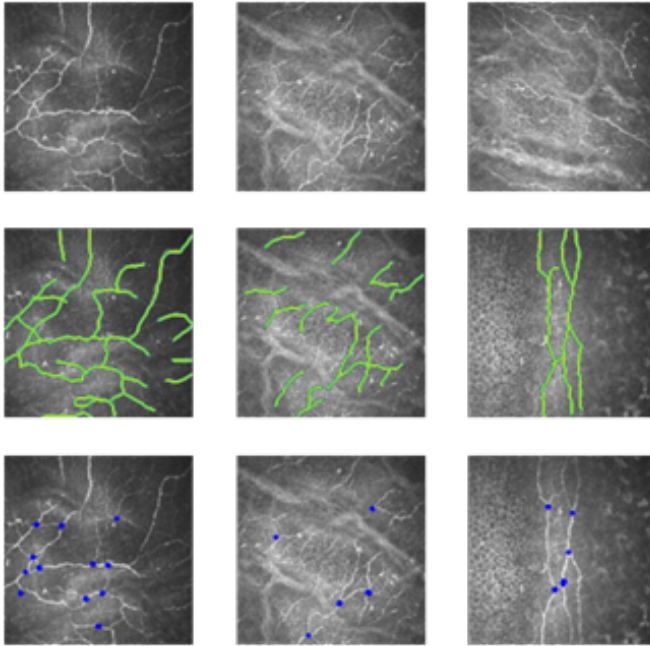


Fig. 4. Confocal Corneal Microscopy (CCM) image showcasing expert-annotated nerve fibre segmentation and corneal nerve branch.

(mIoU) and diagnostic accuracy. For instance, in the Base configuration, HMSViT achieves a 55.76% mIoU versus 53.00% for Swin and 52.00% for HiViT. This superior performance can be attributed to its hierarchical multi-scale design and pooling-based token mixing, which effectively capture fine-grained details while preserving global context with fewer parameters.

Diagnostic Classification: HMSViT demonstrates superior

performance in classifying Healthy Volunteers (HV), Diabetic Patients without Neuropathy (PN−), and with Neuropathy (PN+). The Base configuration reaches a diagnostic accuracy of 70.40%, outperforming Swin (68.42%) and HiViT (67.55%). This improvement is linked to the integration of masked self-supervised learning, which enhances spatial reasoning and feature extraction.

Corneal Nerve fibre Analysis: Table VI provides clinically relevant metrics for corneal nerve fibre length (CNFL) and branch density (CNBD). The Base configuration yields the lowest RMSE and SD values, indicating its superior ability to capture essential features.

Overall, HMSViT exhibits robust performance in both segmentation and diagnosis, leveraging efficient multi-scale feature extraction and advanced self-supervised learning for effective DPN screening.

B. Ablation Study to Evaluate the Impact of Hierarchical Design and Self-Supervised Learning

Table VII summarized the results of these settings in terms of classification accuracy and segmentation performance.

For DPN diagnosis, the results demonstrated that self-supervised learning (SSL) consistently enhanced model performance compared to supervised training alone. Specifically, the model trained with SSL and a hierarchical structure achieved the highest classification accuracy of 70.40%, while supervised learning without the hierarchical structure yielded 65.60% accuracy. This indicates that SSL effectively leverages unlabelled data to improve diagnostic capability. Moreover, incorporating the hierarchical structure provided additional gains, increasing supervised learning accuracy from 65.60% (without hierarchical design) to 66.60% (with hierarchical design).

For nerve segmentation, the segmentation quality measured by mean Intersection over Union (mIoU) improved significantly with both the hierarchical structure and SSL. The supervised model without the hierarchical structure achieved an mIoU of 54.31%, while adding the hierarchical structure increased it to 57.28%. Notably, the combination of SSL and the hierarchical structure resulted in the highest mIoU of 61.34%, underscoring the benefits of integrating multi-scale feature extraction with self-supervised learning.

Model	Size	Channels	Blocks	Param	Nerve Segmentation		Diagnostic classification
					mIoU	Accuracy	Accuracy
Swin	Tiny	[96-192-384-768]	12	29M	49.50%	96.00%	62.34%
HiViT		[96-192-384]		20M	48.00%	95.00%	61.25%
HMSViT		[96-192-384-768]		28M	52.17%	98.50%	64.32%
Swin	Small	[96-192-384-768]	16	50M	51.00%	97.00%	64.32%
HiViT		[96-192-384]		38M	50.00%	96.50%	65.28%
HMSViT		[96-192-384-768]		35M	53.23%	98.50%	67.60%
Swin	Base	[128-256-512-1024]	24	88M	53.00%	97.50%	68.42%
HiViT		[128-256-512]		67M	52.00%	97.00%	67.55%
HMSViT		[128-256-384-512]		52M	55.76%	98.39%	70.40%

TABLE V

PERFORMANCE COMPARISON OF HIERARCHICAL TRANSFORMER-BASED MODELS FOR AUTOMATED CORNEAL NERVE SEGMENTATION AND DIABETIC NEUROPATHY DIAGNOSIS.

HMSViT		Tiny	Small	Base
CNFL	RMSE	501.623	463.471	326.002
	SD	500.63	302.231	271.745
CNBD	RMSE	7.3667	5.1326	4.1603
	SD	6.911	4.3934	4.1652

TABLE VI

PERFORMANCE EVALUATION OF VARIOUS MODEL CONFIGURATIONS OF HMSViT FOR CORNEAL NERVE FIBRE ANALYSIS ON CLINICALLY RELEVANT PARAMETERS, INCLUDING CORNEAL NERVE FIBRE LENGTH (CNFL) AND CORNEAL NERVE BRANCH DENSITY (CNBD).

Diagnostic classification accuracy		
	No Hierarchical	With Hierarchical
Supervised	65.60%	66.60%
Self-supervised	69.40%	70.40%
Corneal nerve segmentation performance		
Supervised	54.31%	57.28%
Self-supervised	55.14%	61.34%

TABLE VII

DIAGNOSTIC CLASSIFICATION ACCURACY AND CORNEAL NERVE SEGMENTATION PERFORMANCE FOR DIFFERENT TRAINING CONFIGURATIONS, ASSESSING THE IMPACT OF HIERARCHICAL DESIGN AND SELF-SUPERVISED LEARNING.

C. Comparison with State-of-the-Art Methods for Segmentation

Models	Backbone	Self-supervised	Param	mIoU (%)
DPT [24]	ViT	None	97M	54.31
PoolFormer [40]	HiViT	None	77M	55.32
SegFormer [41]	HiViT	None	85M	57.39
MOCOV3+ViT	ViT	MOCOV3	86M	56.62
MAE+ViT	ViT	MAE	86M	57.08
MAE+HiViT	HiViT	MAE modified	73M	61.06
MixMIM [38]	HiViT	MAE modified	88M	60.86
Fast-iTPN [39]	HiViT	MAE modified	79M	61.25
Proposed method	HMSViT	MAE modified	68M	61.34

TABLE VIII

PERFORMANCE COMPARISON OF BACKBONE ARCHITECTURES AND SELF-SUPERVISED LEARNING METHODS IN NERVE SEGMENTATION.

In Table VIII, we compared the performance and computational efficiency of state-of-the-art vision transformer-based segmentation models. The DPT model, built on a standard Vision Transformer architecture with 97M parameters, achieved an mIoU of 54.31%. In contrast, hierarchical models like PoolFormer (77M parameters) and SegFormer (85M parameters) showed modest improvements, reaching mIoU scores

of 55.32% and 57.39%, respectively.

Notably, the application of self-supervised learning further enhanced performance. The models utilizing MAE-based techniques, such as MAE+ViT (86M parameters, mIoU: 57.08%) and MAE+HiViT (73M parameters, mIoU: 61.06%), benefited from the integration of a hierarchical design. Similarly, Fast-iTPN, incorporating a modified MAE framework with 79M parameters, achieves an mIoU of 61.25%.

Our proposed HMSViT achieved the highest mIoU of 61.34% with only 68M parameters, ensuring a strong balance between accuracy and efficiency. Its novel hierarchical multi-scale architecture and optimised self-supervised pretraining enhanced both fine-grained details and global context. These features made it well-suited for complex medical imaging tasks.

VI. DISCUSSION

This approach addressed key challenges in medical imaging, where limited labelled data often restricts deep learning applications. Unlike previous models that relied on large annotated datasets, our SSL approach enabled efficient learning from limited labelled data. This was especially valuable for high-dimensional corneal confocal microscopy (CCM) images, which were often scarce. Comparisons with state-of-the-art methods highlighted HMSViT's superior performance over models using only hierarchical vision transformers or convolutional neural networks. By leveraging multi-scale feature extraction, our model captured both fine-grained local details and broader structural patterns, enhancing segmentation accuracy and improving diagnostic reliability. The use of multi-scale feature extraction enabled the proposed model to discern both fine-grained local features and broader structural patterns, improving segmentation accuracy and facilitating the extraction of clinically relevant parameters, such as corneal nerve fibre length (CNFL) and branch density.

One of the key innovations of the HMSViT model is its ability to capture hierarchical multi-scale features, effectively combining local and global contextual information. This capability is crucial in medical imaging tasks where both fine-grained details and broader structural patterns contribute to accurate diagnosis. As illustrated in Figure 5, the hierarchical feature extraction approach enabled the model to enhance segmentation accuracy, as evidenced by its superior performance in mean Intersection over Union (mIoU) compared to existing

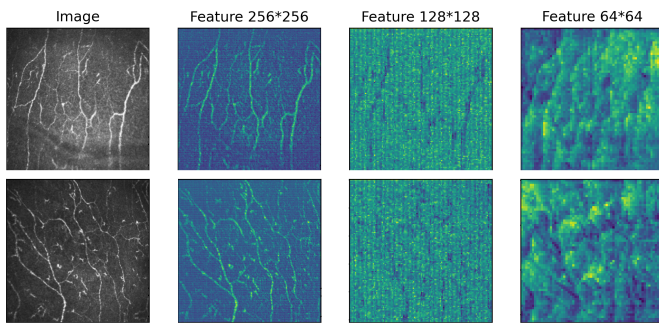


Fig. 5. Multi scale feature extraction from the proposed HMSViT.

models. The hierarchical nature of the HMSViT allowed for better retention of nerve fibre structure and branching patterns, ensuring more precise morphological assessments. Another innovation in HMSViT is its streamlined design featuring a pooling-based token mixer, which minimizes architectural complexity while maintaining robust performance. This simplicity is key to the model’s computational efficiency. Notably, HMSViT achieved an mIoU of 61.34% using only 68M parameters, outperforming more complex architectures that required significantly higher computational resources. Such efficiency is critical for deployment in clinical environments where processing speed and resource constraints are paramount. A significant challenge in medical imaging is the scarcity of labelled datasets, which limits the performance of supervised deep learning models. The proposed HMSViT mitigates this limitation by leveraging self-supervised learning, which enables the model to learn meaningful representations from large amounts of unlabelled data. The ablation study results confirmed that the addition of self-supervised learning significantly enhanced both segmentation and classification performance. Notably, the model trained with SSL and the hierarchical structure achieved the highest classification accuracy of 70.40% and an mIoU of 61.34%. These improvements underscore the importance of SSL in enabling efficient feature learning, reducing reliance on expensive manual annotations.

A direct comparison of the proposed model with other state-of-the-art methods highlights its superior performance. While previous hierarchical vision transformers such as HiViT and Fast-iTPN achieved competitive results, the HMSViT surpassed these models in segmentation performance due to its optimized pyramid structure and modified Masked Auto-encoder (MAE) approach. The ability to outperform models that rely solely on hierarchical architectures or traditional convolutional networks demonstrates the effectiveness of integrating SSL with multi-scale feature extraction. The proposed approach not only improves segmentation quality but also enhances diagnostic accuracy, reinforcing its potential for real-world clinical applications.

Furthermore, the ability to quantify clinically relevant parameters such as Corneal Nerve fibre Length (CNFL) and Corneal Nerve Branch Density (CNBD) demonstrates the practical utility of the HMSViT. By extracting these biomarkers with high precision, the model supports objective and reproducible assessments, which are critical for tracking disease

progression and evaluating treatment efficacy.

Despite its advantages, the proposed approach has certain limitations. While HMSViT has shown strong performance on the available dataset, its generalisability to larger and more diverse datasets remains to be validated. Future studies should explore the model’s robustness across different populations, imaging conditions, and disease severities to ensure broad applicability. Additionally, although self-supervised learning significantly reduces the need for annotated data, further enhancements in unsupervised learning strategies could be explored to maximize performance. The integration of contrastive learning techniques or multi-modal learning approaches incorporating additional clinical data (e.g., patient history, genetic markers) could further enhance the model’s diagnostic capabilities.

VII. CONCLUSION

In this work, we presented HMSViT—a Hierarchical Multi-Scale Vision Transformer that integrates a novel block masked self-supervised learning strategy with a streamlined hierarchical architecture. By combining a pooling-based hierarchical design with a multi-scale decoder, HMSViT successfully captures both fine-grained local details and broader global contexts from corneal confocal microscopy images. Our extensive experiments on clinical datasets demonstrated that HMSViT achieves state-of-the-art performance, with a mean Intersection over Union (mIoU) of 61.34% for corneal nerve segmentation and a diagnostic accuracy of 70.40% for diabetic peripheral neuropathy classification. Ablation studies confirmed that the improvements are driven by both the block masked self-supervised pretraining and the hierarchical feature extraction, allowing HMSViT to outperform competitive models like the Swin Transformer and HiViT while utilizing fewer parameters.

Looking ahead, future work will focus on validating the model on larger and more diverse datasets to ensure robustness across different imaging conditions and patient populations. We also plan to enhance the model’s interpretability and explore complementary self-supervised techniques—such as contrastive and multimodal learning, to further improve diagnostic performance and facilitate integration into clinical workflows.

REFERENCES

- [1] Z. Iqbal, S. Azmi, R. Yadav, M. Ferdousi, M. Kumar, D. J. Cuthbertson, J. Lim, R. A. Malik, and U. Alam, “Diabetic peripheral neuropathy: Epidemiology, diagnosis, and pharmacotherapy,” *Clinical Therapeutics*, vol. 40, no. 6, pp. 828–849, jun 1 2018.
- [2] J. Burgess, B. Frank, A. Marshall, R. S. Khalil, G. Ponirakis, I. N. Petropoulos, D. J. Cuthbertson, R. A. Malik, and U. Alam, “Early detection of diabetic peripheral neuropathy: A focus on small nerve fibres,” *Diagnostics*, vol. 11, no. 2, p. 165, jan 24 2021, PMID: 33498918 PMID: PMC7911433.
- [3] X. Chen, J. Graham, M. A. Dabbah, I. N. Petropoulos, M. Tavakoli, and R. A. Malik, “An automatic tool for quantification of nerve fibers in corneal confocal microscopy images,” *IEEE Transactions on Biomedical Engineering*, vol. 64, no. 4, pp. 786–794, 2016, publisher: IEEE.
- [4] H. Gad, I. N. Petropoulos, A. Khan, G. Ponirakis, R. MacDonald, U. Alam, and R. A. Malik, “Corneal confocal microscopy for the diagnosis of diabetic peripheral neuropathy: A systematic review and metaanalysis,” *Journal of Diabetes Investigation*, vol. 13, no. 1, pp. 134–147, 1 2022, PMID: 34351711 PMID: PMC8756328.

- [5] I. N. Petropoulos, G. Ponirakis, M. Ferdousi, S. Azmi, A. Kalteniece, A. Khan, H. Gad, B. Bashir, A. Marshall, A. J. M. Boulton, H. Soran, and R. A. Malik, "Corneal confocal microscopy: A biomarker for diabetic peripheral neuropathy," *Clinical Therapeutics*, vol. 43, no. 9, pp. 1457–1475, 9 2021, pMID: 33965237.
- [6] D. R. Sarvamangala and R. V. Kulkarni, "Convolutional neural networks in medical image understanding: a survey," *Evolutionary Intelligence*, vol. 15, no. 1, pp. 1–22, 2022, pMID: 33425040 PMID: PMC7778711.
- [7] B. M. Williams, D. Borroni, R. Liu, Y. Zhao, J. Zhang, J. Lim, B. Ma, V. Romano, H. Qi, and M. Ferdousi, "An artificial intelligence-based deep learning algorithm for the diagnosis of diabetic neuropathy using corneal confocal microscopy: a development and validation study," *Diabetologia*, vol. 63, no. 2, pp. 419–430, 2020, publisher: Springer.
- [8] A. Dosovitskiy, L. Beyer, A. Kolesnikov, D. Weissenborn, X. Zhai, T. Unterthiner, M. Dehghani, M. Minderer, G. Heigold, S. Gelly, J. Uszkoreit, and N. Houlsby, "An image is worth 16x16 words: Transformers for image recognition at scale," *arXiv:2010.11929 [cs]*, oct 22 2020, arXiv: 2010.11929. [Online]. Available: <http://arxiv.org/abs/2010.11929>
- [9] R. Azad, A. Kazerouni, M. Heidari, E. K. Aghdam, A. Molaei, Y. Jia, A. Jose, R. Roy, and D. Merhof, "Advances in medical image analysis with vision transformers: A comprehensive review," *Medical Image Analysis*, vol. 91, p. 103000, 1 2024, pMID: 37883822.
- [10] S. K. Zhou, H. Greenspan, C. Davatzikos, J. S. Duncan, B. van Ginneken, A. Madabhushi, J. L. Prince, D. Rueckert, and R. M. Summers, "A review of deep learning in medical imaging: Imaging traits, technology trends, case studies with progress highlights, and future promises," *Proceedings of the IEEE. Institute of Electrical and Electronics Engineers*, vol. 109, no. 5, pp. 820–838, 5 2021, pMID: 37786449 PMID: PMC10544772.
- [11] Z. Liu, Y. Lin, Y. Cao, H. Hu, Y. Wei, Z. Zhang, S. Lin, and B. Guo, "Swin transformer: Hierarchical vision transformer using shifted windows," *arXiv:2103.14030 [cs]*, mar 25 2021, arXiv: 2103.14030. [Online]. Available: <http://arxiv.org/abs/2103.14030>
- [12] X. Zhang, Y. Tian, W. Huang, Q. Ye, Q. Dai, L. Xie, and Q. Tian, "Hivit: Hierarchical vision transformer meets masked image modeling," may 30 2022, arXiv:2205.14949 [cs]. [Online]. Available: <http://arxiv.org/abs/2205.14949>
- [13] P. Saedi, I. Petersohn, P. Salpea, B. Malanda, S. Karuranga, N. Unwin, S. Colagiuri, L. Guariguata, A. A. Motala, K. Ogurtsova *et al.*, "Global and regional diabetes prevalence estimates for 2019 and projections for 2030 and 2045: Results from the international diabetes federation diabetes atlas," *Diabetes research and clinical practice*, vol. 157, p. 107843, 2019.
- [14] P. Sharma, "Diabetic peripheral neuropathy," in *Rehabilitation in Diabetic Peripheral Neuropathy*. Springer, 2025, pp. 1–19.
- [15] A. J. Boulton, A. I. Vinik, J. C. Arezzo, V. Bril, E. L. Feldman, R. Freeman, R. A. Malik, R. E. Maser, J. M. Sosenko, and D. Ziegler, "Diabetic neuropathies: a statement by the american diabetes association," *Diabetes care*, vol. 28, no. 4, pp. 956–962, 2005, publisher: Am Diabetes Assoc.
- [16] J. R. Ball, B. T. Miller, and E. P. Balogh, "Improving diagnosis in health care," 2015.
- [17] F. G. Preston, Y. Meng, J. Burgess, M. Ferdousi, S. Azmi, I. N. Petropoulos, S. Kaye, R. A. Malik, Y. Zheng, and U. Alam, "Artificial intelligence utilising corneal confocal microscopy for the diagnosis of peripheral neuropathy in diabetes mellitus and prediabetes," *Diabetologia*, vol. 65, no. 3, pp. 457–466, 3 2022, pMID: 34806115 PMID: PMC8803718.
- [18] Y. Meng, F. G. Preston, M. Ferdousi, S. Azmi, I. N. Petropoulos, S. Kaye, R. A. Malik, U. Alam, and Y. Zheng, "Artificial intelligence based analysis of corneal confocal microscopy images for diagnosing peripheral neuropathy: a binary classification model," *Journal of Clinical Medicine*, vol. 12, no. 4, p. 1284, 2023, publisher: MDPI.
- [19] Q. Qiao, J. Cao, W. Xue, J. Qian, C. Wang, Q. Pan, B. Lu, Q. Xiong, L. Chen, and X. Hou, "Deep learning-based automated tool for diagnosing diabetic peripheral neuropathy," *Digital Health*, vol. 10, p. 20552076241307573, dec 25 2024, pMID: 39741986 PMID: PMC11686633.
- [20] K. Teh, I. D. Wilkinson, G. P. Sloan, S. Tesfaye, and D. Selvarajah, "455-p: Artificial intelligence approach to treatment classification in painful diabetic neuropathy," *Diabetes*, vol. 71, no. Supplement_1, 2022.
- [21] W. Li, Z. Tang, L. Zhao, W. Tian, and T. Qi, "Context encoder network with channel-wise attention mechanism for nerve fibers detection in corneal confocal microscopy images," pp. 1–6, 2022.
- [22] W. Chen, D. Liao, Y. Deng, and J. Hu, "Development of a transformer-based deep learning algorithm for diabetic peripheral neuropathy classification using corneal confocal microscopy images," *Frontiers in Cell and Developmental Biology*, vol. 12, p. 1484329, 2024, publisher: Frontiers Media SA.
- [23] H. Touvron, M. Cord, M. Douze, F. Massa, A. Sablayrolles, and H. Jégou, "Training data-efficient image transformers & distillation through attention," jan 15 2021, arXiv:2012.12877 [cs]. [Online]. Available: <http://arxiv.org/abs/2012.12877>
- [24] R. Ranftl, A. Bochkovskiy, and V. Koltun, "Vision transformers for dense prediction," pp. 12 179–12 188, 2021.
- [25] W. Wang, E. Xie, X. Li, D.-P. Fan, K. Song, D. Liang, T. Lu, P. Luo, and L. Shao, "Pyramid vision transformer: A versatile backbone for dense prediction without convolutions," pp. 568–578, 2021.
- [26] Y. Li, C.-Y. Wu, H. Fan, K. Mangalam, B. Xiong, J. Malik, and C. Feichtenhofer, "Mvitv2: Improved multiscale vision transformers for classification and detection," pp. 4804–4814, 2022.
- [27] C. Ryali, Y.-T. Hu, D. Bolya, C. Wei, H. Fan, P.-Y. Huang, V. Aggarwal, A. Chowdhury, O. Poursaeed, J. Hoffman *et al.*, "Hiera: A hierarchical vision transformer without the bells-and-whistles," pp. 29 441–29 454, 2023.
- [28] A. Khan, A. Sohail, M. Fiaz, M. Hassan, T. H. Afridi, S. U. Marwat, F. Munir, S. Ali, H. Naseem, M. Z. Zaheer, K. Ali, T. Sultana, Z. Tanoli, and N. Akhter, "A survey of the self supervised learning mechanisms for vision transformers," oct 31 2024, arXiv:2408.17059 [cs]. [Online]. Available: <http://arxiv.org/abs/2408.17059>
- [29] S. Albelwi, "Survey on self-supervised learning: auxiliary pretext tasks and contrastive learning methods in imaging," *Entropy*, vol. 24, no. 4, p. 551, 4 2022, number: 4 publisher: Multidisciplinary Digital Publishing Institute.
- [30] C. Doersch, A. Gupta, and A. A. Efros, "Unsupervised visual representation learning by context prediction," jan 16 2016, arXiv:1505.05192 [cs]. [Online]. Available: <http://arxiv.org/abs/1505.05192>
- [31] D. Pathak, P. Krahenbuhl, J. Donahue, T. Darrell, and A. A. Efros, "Context encoders: Feature learning by inpainting," pp. 2536–2544, 2016.
- [32] M. Noroozi and P. Favaro, "Unsupervised learning of visual representations by solving jigsaw puzzles," in *European conference on computer vision*. Springer, 2016, pp. 69–84.
- [33] S. Gidaris, P. Singh, and N. Komodakis, "Unsupervised representation learning by predicting image rotations," *arXiv preprint arXiv:1803.07728*, 2018.
- [34] T. Chen, S. Kornblith, M. Norouzi, and G. Hinton, "A simple framework for contrastive learning of visual representations," pp. 1597–1607, 2020.
- [35] K. He, H. Fan, Y. Wu, S. Xie, and R. Girshick, "Momentum contrast for unsupervised visual representation learning," pp. 9729–9738, 2020.
- [36] K. He, X. Chen, S. Xie, Y. Li, P. Dollár, and R. Girshick, "Masked autoencoders are scalable vision learners," in *Proceedings of the IEEE/CVF conference on computer vision and pattern recognition*, 2022, pp. 16 000–16 009.
- [37] C. Wei, H. Fan, S. Xie, C.-Y. Wu, A. Yuille, and C. Feichtenhofer, "Masked feature prediction for self-supervised visual pre-training," in *Proceedings of the IEEE/CVF conference on computer vision and pattern recognition*, 2022, pp. 14 668–14 678.
- [38] J. Liu, X. Huang, J. Zheng, Y. Liu, and H. Li, "Mixmae: Mixed and masked autoencoder for efficient pretraining of hierarchical vision transformers," in *Proceedings of the IEEE/CVF Conference on Computer Vision and Pattern Recognition*, 2023, pp. 6252–6261.
- [39] Y. Tian, L. Xie, J. Qiu, J. Jiao, Y. Wang, Q. Tian, and Q. Ye, "Fast-iptn: Integrally pre-trained transformer pyramid network with token migration," *IEEE Transactions on Pattern Analysis and Machine Intelligence*, 2024.
- [40] W. Yu, M. Luo, P. Zhou, C. Si, Y. Zhou, X. Wang, J. Feng, and S. Yan, "Metaformer is actually what you need for vision," jul 4 2022, arXiv:2111.11418 [cs]. [Online]. Available: <http://arxiv.org/abs/2111.11418>
- [41] E. Xie, W. Wang, Z. Yu, A. Anandkumar, J. M. Alvarez, and P. Luo, "Segformer: Simple and efficient design for semantic segmentation with transformers," oct 28 2021, arXiv:2105.15203 [cs]. [Online]. Available: <http://arxiv.org/abs/2105.15203>
- [42] X. Chen, S. Xie, and K. He, "An empirical study of training self-supervised vision transformers," pp. 9640–9649, 2021.